The AAPS Journal 2005; 7 (1) Article 24 (http://www.aapsj.org).

A Random Sampling Approach for Robust Estimation of Tissue-to-Plasma Ratio From Extremely Sparse Data

Submitted: May 13, 2004; Accepted: July 16, 2004; Published: September 2, 2005

Hui-May Chu and Ene I. Ette

Department of Clinical Pharmacology, Vertex Pharmaceuticals Inc, 130 Waverly Street, Cambridge, MA 02139-4242

ABSTRACT

This study was performed to develop a new nonparametric approach for the estimation of robust tissue-to-plasma ratio from extremely sparsely sampled paired data (ie, one sample each from plasma and tissue per subject). Tissue-to-plasma ratio was estimated from paired/unpaired experimental data using independent time points approach, area under the curve (AUC) values calculated with the naive data averaging approach, and AUC values calculated using sampling based approaches (eg, the pseudoprofile-based bootstrap [PpbB] approach and the random sampling approach [our proposed approach]). The random sampling approach involves the use of a 2-phase algorithm. The convergence of the sampling/resampling approaches was investigated, as well as the robustness of the estimates produced by different approaches. To evaluate the latter, new data sets were generated by introducing outlier(s) into the real data set. One to 2 concentration values were inflated by 10% to 40% from their original values to produce the outliers. Tissue-to-plasma ratios computed using the independent time points approach varied between 0 and 50 across time points. The ratio obtained from AUC values acquired using the naive data averaging approach was not associated with any measure of uncertainty or variability. Calculating the ratio without regard to pairing yielded poorer estimates. The random sampling and pseudoprofile-based bootstrap approaches yielded tissue-to-plasma ratios with uncertainty and variability. However, the random sampling approach, because of the 2-phase nature of its algorithm, yielded more robust estimates and required fewer replications. Therefore, a 2-phase random sampling approach is proposed for the robust estimation of tissue-to-plasma ratio from extremely sparsely sampled data.

KEYWORDS: paired extremely sparsely sampled data, tissue-to-plasma ratio, random sampling approach, pseudoprofile-based approach, convergence, robustness

Corresponding Author: Hui-May Chu, Department of Clinical Pharmacology, Vertex Pharmaceuticals Inc, 130 Waverly Street, Cambridge, MA 02139-4242; Tel: (617) 444-6398; Fax: (617) 444-6713; E-mail: Hui-May_Chu@vrtx.com

INTRODUCTION

Toxicokinetic and pharmacokinetic research is characterized by some uncertainty regarding the process studied and significant variation in the concentration measurements obtained. Variability in pharmacokinetic parameters among homogeneous strains of small laboratory animals has been reported to be between 30% and 50% in some cases[1,2] In addition to the inherent variability of the biological system, there is the uncertainty associated with the assay and process noise.

The number of samples that can be obtained per subject is limited to one sample per subject in most rodent toxicokinetic studies. The fact is that for small laboratory animals, the periods between successive sampling times are simply not long enough to allow for sufficient recovery. A major disadvantage of this sampling scheme is that intraindividual concentration time profiles are unavailable. This poses a data analysis challenge because the one sample per subject data constitute the extreme case of sparsely sampled pharmacokinetic data, hence extremely sparse data, with independent observations over time. The situation is complicated when tissue sampling (eg, in tissue distribution studies) is involved, and the ratio of tissue to plasma concentrations is the object of the investigation. Equally, only one tissue sample/subject is obtained in such studies because the animal is usually killed.

Tissue-to-plasma ratio is commonly determined from the ratio of average concentrations at specified time points. It is not uncommon, in practice, for the ratios to be calculated at selected time points corresponding to peak and trough concentrations, and the variations in the ratios are usually very large. This finding could be attributed in part to the variations in the concentrations and a lack of accounting for the correlation in observations from the biological matrices sampled from each subject.

Occasionally tissue-to-plasma ratio is calculated using area under the concentration curves (AUCs) calculated from mean profiles using the noncompartmental approach. These ‘‘composite’’ AUCs are usually computed from data that are averaged at each time point (naive data averaging approach) using the trapezoidal rule. The tissue-to-plasma ratios computed using either average concentrations at specified time points or composite AUC values are usually reported without regard to the correlation structure in the data, and no measures of dispersion and uncertainty associated

with them. In this study, we present the results of an investigation into the estimation of robust tissue-to-plasma ratio in a drug development setting using a new nonparametric random sampling approach.

METHODS

Data Set

Since the objective of this report is the development of a methodology for estimating robust tissue-to-plasma ratio in a drug development setting, such details as are necessary for understanding the proposed methodology are presented. It is important to note that in drug development pragmatism, efficiency, and effectiveness are major considerations.

A toxicokinetic study was performed to determine the tissue-to-plasma ratio of a drug. An oral dose of the drug was administered to 18 rats, and each animal was killed at 1 of 6 specified time points: 0.5, 1, 2, 4, 6, and 8 hours. Therefore, each animal had only 1 pair of concentrations, 1 each from plasma and tissue, respectively. Table 1 shows the data set from the study used in our investigation. The effect of correlation structure in the data set is also of interest. Thus, we investigated the effect of maintaining or breaking the relationship between tissue and plasma concentrations within the same animal, using both paired and unpaired tissue and plasma data to evaluate the effect on the robustness of estimation of tissue-to-plasma ratio.

Data Analyses Approaches

We have taken a very practical approach in addressing the computation of tissue-to-plasma ratio in a drug development setting. Thus, approaches that are commonly used in practice (ie, the naive data averaging and ratios of concentrations by time point approaches) for computing tissue-to-plasma ratio were employed in this investigation and compared with our proposed methodology—the random sampling approach. Since our approach is a sampling-based approach, we have included a comparison of the performance of our approach with another sampling-based approach reported in the literature, the PpbB,[3] in the estimation of tissue-to-plasma ratio. First, we discuss the naive data averaging approach followed by a discussion of the random sampling approach, and then the PpbB approach.

Naive Data Averaging Approach

The approach involves computing the average value of the data for each sampling time k

$$\overline{C}_k = \frac{1}{I}\sum_{i=1}^{I} C_{ik} \qquad (1)$$

for $i = 1, \ldots, I,$ where I is the standard number of individual subject data at time point k. The averaging of data across subjects is a common practice owing to the assumption that all concentrations at each time point have been measured under identical conditions.

Thus, tissue-to-plasma ratio is estimated independently for each time point using the averaged concentration at each time point. Alternatively, the noncompartmental AUC, actually the composite AUC, can be estimated using the trapezoidal rule. From this point, the use of the term ''naive data averaging approach'' will be reserved for estimation of AUC. The term ''unpaired independent time points approach'' will be reserved for use in cases where tissue-to-plasma ratio is calculated at each time point using a measure of central tendency (mean or median) of the measured concentrations without regard to the correlation structure in the observations. The term ''paired independent time points'' approach will be used when the pairing of observations is taken into account in the calculation of the tissue-to-plasma concentration ratio at each time point.

Random Sampling Approach

To implement the random sampling (RS) approach, we first generate the population sampling pool that comprises a large set of individual pharmacokinetic (PK) profiles based on the empirical data by resampling with replacement.

Table 1. Data Set From an Oral Toxicokinetic Study*

	Time Point (hour)					
Biological Matrix	**0.5**	**1**	**2**	**4**	**6**	**8**
Plasma	0.18	0.13	0.12	0.04	0.00	0.01
Tissue	9.05	1.76	1.26	0.18	0.02	0.42
Plasma	0.18	0.14	0.11	0.03	0.05	0.00
Tissue	5.24	1.65	1.67	0.64	0.28	0.07
Plasma	0.17	0.18	0.05	0.02	0.02	0.00
Tissue	2.92	4.18	0.74	0.19	0.00	0.10

*Each cell represents a pair of values from 1 animal. There are 18 animals in total.

This potential population pool contains M_1 copies of PK profiles for each subject to ensure equal opportunity for each subject to be resampled for the next step. Next, M_2 copies of the virtual study are drawn from the population pool, and then any function of interest is computed from the virtual study level. Figure 1 is a schematic chart illustrating the RS approach. The RS algorithm, therefore, is defined in 2 phases.

Phase 1: Setting up the Population Sampling Pool by Generating Individual Subject Sampling Pools

Phase 1 is done by constructing the individual level sampling pool (ie, the concentration values for the *i*th subject at *r*th replicate resampling (C^*_{ir})). The steps to do this are as follows:

(1) For the *ith* subject with datum observed at time point *w*, randomly resample M_1 times with replacement from the available values independently at each time point that the subject had no observation. For a subject that has *w*th time point observation, for example, the concentration values are to be resampled (ie, plasma and tissue concentrations) at other *k* time points C^*_{ikr}, (where, $k = 1, \ldots, K$, but $k \neq w$, and $r = 1, \ldots, M_1$) to create a ''complete profile'' encompassing all sample points, including the observed C_{iwr} and the resampled vector C^*_{ikr}. More specifically, $C^*_{i..}$, M_1 replicates of ''complete profiles'' for the *i*th subject, can be expressed as the matrix below:

$$C^*_{i..} = \begin{bmatrix} c^*_{i11} & \cdots & c_{iw1} & \cdots & c^*_{iK1} \\ \cdots & \cdots & \cdots & \cdots & \cdots \\ c^*_{i1M_1} & \cdots & c_{iwM_1} & \cdots & c^*_{iKM_1} \end{bmatrix}.$$

Each row represents one profile encompassing all sample/time points. Each column is M_1 copy of the same time point.

(2) Repeat (1) of Phase 1 to construct the individual profile pool for each subject.

(3) Calculate functions of interest from each profile (eg, AUC, C_{max}).

The population sampling pool of complete profiles is now ready to be sampled for the next phase of virtual study resampling.

Phase 2: Generation of Samples at the Study Level

(1) Draw M_2 copies of size N (where N is the sample size, total number of animals, in the real study) of functions of interest from the population sampling pool obtained from Phase 1.

(2) Calculate the summary statistics (eg, quantiles, mean, and median) of the function of interest from each virtual study obtained from (1) of Phase 2.

(3) Derive the summary statistics of required parameters across virtual studies with their associated standard deviations.

The Bootstrap Technology

The principle of the bootstrap is to repeatedly generate pseudosamples distributed according to the same distribution as the original sample.[4,5] The original data set consists

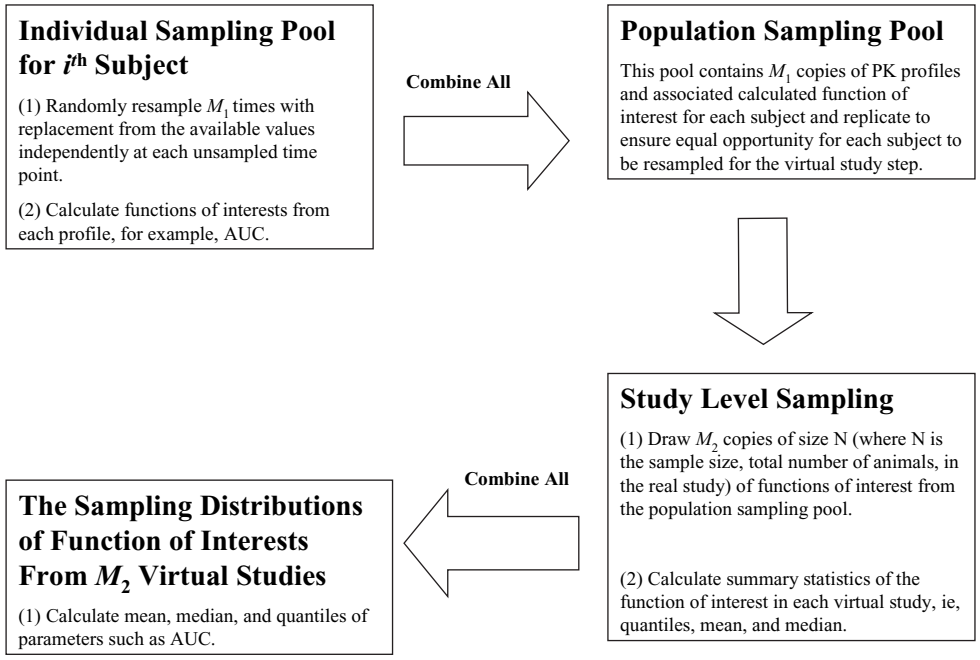

Figure 1. A schematic chart for random sampling approach.

Table 2. Tissue-to-Plasma Ratios Calculated Using the Unpaired Independent Time Points Approach*

	Time Point (hour)					
Tissue/Plasma Ratio	**0.5**	**1**	**2**	**4**	**6**	**8**
Median	30	14	14	10	#DIV/0	#DIV/0
Mean	32	16	13	12	#DIV/0	#DIV/0

*#DIV/0 indicates the denominator (plasma concentration) of the ratio is 0 (or below the quantifiable limit (BQL)).

of an independent and identically distributed (iid) sample of size N from an unknown probability distribution. Original distribution F, though unknown, may be replaced by the empirical distribution of the sample denoted by $\hat{F}^*$.

In this setting, let x_i represent the observed data of ith subject in a training data set, such that x_i includes all the observed concentrations. The entire training data set (empirical sample) may be represented by the set of vectors, $X = (x_1, \ldots, x_N)$. A bootstrap sample is generated as follows:

(1) Repeated random sampling and replacement of an N-pseudosample (x_i*), which is an iid sample from the empirical distribution of the vector X. Every subject has equal probability of being sampled with each repetition.

(2) The sampling is repeated until the bootstrap sample also consists of N (the original sample size) vectors, $X_B = (x_1^*, x_2^*, \ldots, x_N^*)$. Each x* represents data from a subject randomly selected.

Pseudoprofile-based Bootstrap

The PpbB approach[3] generates estimates of both the distributions of the raw data and the corresponding measures of variability. The term ''pseudoprofile'' was applied to the information obtained when one sample is obtained per animal but several animals are sampled at each of several times postdose.

Bootstrap resampling is performed twice within the PpbB approach to generate PK pseudoprofiles from which the function of interest is estimated. More specifically, the following scheme is adopted for the b_1th replicate at each time point:

(1) Resample with replacement at one concentration, denoted as $C^*_{b_1}(t_k)$ at time t_k for $k = 1$ to K from the respective concentration vectors and keep K concentrations $c^*_{b_1}(t_k), k = 1, \cdots, K$.

(2) Construct a pseudoprofile that is $c^*_{b_1} = \{c^*_{b_1}(t_1), c^*_{b_1}(t_2), \cdots, c^*_{b_1}(t_{k-1}), c^*_{b_1}(t_k)\}$.

(3) Repeat (1) and (2) B_1 times to generate a PK pseudoprofile pool $\hat{F}^*$ an estimate of the distribution F.

(4) Calculate a function of interest from each pseudoprofile (ie, AUC, C_{max}).

(5) Perform B_2 times Bootstrap resampling with replacement from this empirical distribution $\hat{F}^*$ with sample size $\bar{n}$ each, where $\bar{n}$ is the average number of concentration replicates, and the corresponding parameter for each $b_2 = 1, \cdots, B_2$ is estimated.

(6) Calculate the bootstrap estimates of the mean parameter and its standard deviation.

Since the focus of this study is on the RS approach as the proposed methodology for estimating tissue-to-plasma ratio, with its performance being compared with the PpbB

Table 3. Tissue-to-Plasma Ratios Calculated Using the Paired Independent Time Points Approach*

	Ratios				
Time (hours)	**Minimum**	**Q1**	**Mean**	**Q3**	**Maximum**
0.5	17	23.4	32.3	40	50.3
1	12.2	13.2	16.4	18.5	23
2	10.3	12	13.4	14.9	16
4	5.2	7.4	11.8	15.2	20.7
6	0	1.5	2.9	4.4	5.9
8	32.6	32.6	32.6	32.6	32.6
All time points	0	10	17.4	21.8	50.3

*Q1 indicates first quartile and Q3, third quartile.

Table 4. Tissue-to-Plasma Ratios Calculated from AUC Values Obtained via the Naive Data Averaging Approach*

Central Tendency	Plasma AUC	Tissue AUC	Tissue-to-Plasma AUC Ratio
Mean	0.45	7.62	17.05

*AUC indicates area under the curve.

approach, occasional references are made to the naive data averaging and independent time points approaches because of their use in common practice. All methods were implemented in the statistical software, S-Plus, Version 6.02 (Insightful, Seattle, WA).

Convergence

Convergence was determined for both RS and PpbB approaches. That is, the number of replications (ie, the number of times the sampling/resampling has to be repeated) needed for stable estimates of tissue-to-plasma AUC ratio (TPAR) to be obtained were determined for both methods. An empirical approach was used to determine convergence (see the ''Convergence'' subsection under ''Results'').

Outlier Effect

To investigate the effect of outliers on the robustness with which TPAR was estimated with naive averaging, RS, and PpbB approaches, new data sets were simulated by introducing outlier(s) into the data set. The scenarios we chose can be mapped as a grid (2 × 4 table) (ie, 1 or 2 outliers produced by inflating the higher tissue concentration time points by 10%, 20%, 30%, or 40%). The higher tissue concentration time points were defined as concentrations obtained within 4 hours postdose. These concentrations were randomly chosen in each replication. The outliers were introduced in the region of the concentration time profile (ie, around the higher concentrations), where they were likely to produce maximum effect.

RESULTS

Traditional Naive Data Averaging Approach Incorporating Independent Time Points Approaches

The results of tissue-to-plasma ratio values obtained with 3 approaches: (1) unpaired independent time points approach, (2) paired independent time points approach, and (3) naive data averaging approach (ie, TPAR calculated from AUC computed from averaged concentration data), are presented in Tables 2, 3, and 4. Table 2 illustrates ratios obtained across time points by calculating the mean and median for each time point independently for tissue and plasma. There is no measure of variability around each time point, as expected. When zero was returned for plasma concentration (eg, 6- and 8-hour time points in Table 2) because the levels were not quantifiable or below the limit of quantification, the zero divisor of the ratio yielded the result ''#DIV/0.'' Such an outcome cannot be interpreted and is usually discarded in the presentation of results with the independent time points approach. Table 3 contains summary statistics of paired tissue-to-plasma ratios obtained with the paired independent time points approach. The tissue-to-plasma ratios by time point can vary from 0 to 50.3 across different time points, as shown in the last row of Table 3. Table 4 contains the TPAR derived by calculating the mean AUC values using the naive data averaging approach across time points for both tissue and plasma without regard to the correlation structure in the data. As expected, there is also no measure of variability around TPAR obtained with the naive data averaging method.

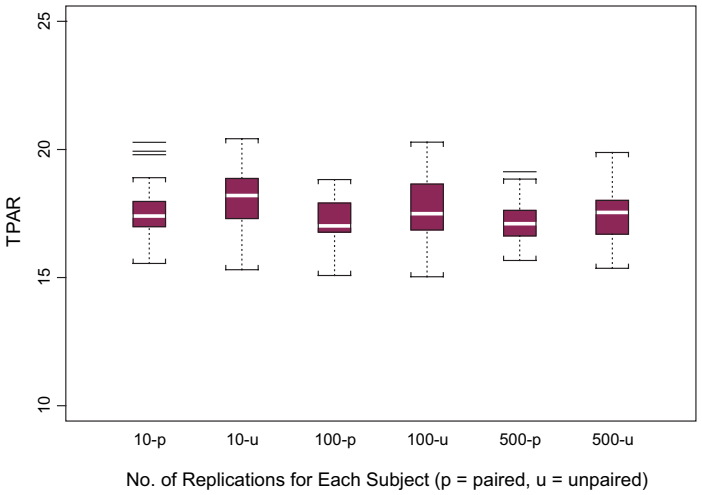

Figure 2. Computation of TPAR from paired and unpaired data using the random sampling approach. This illustrates the paired vs unpaired TPAR mean distributions over 50 virtual studies at different replication levels. The line inside the box represents the median, and the box represents the limits of the middle half of the data. The range of the box, from the first quartile (Q1) to the third quartile (Q3), is called the Inter-Quartile range (IQR). The standard span of the data are defined within the range from Q1–1.5 × IQR to Q3+1.5 × IQR. Whiskers, the dotted line, are drawn to the nearest value not beyond the range of the standard span; points beyond (outside values) are drawn individually.

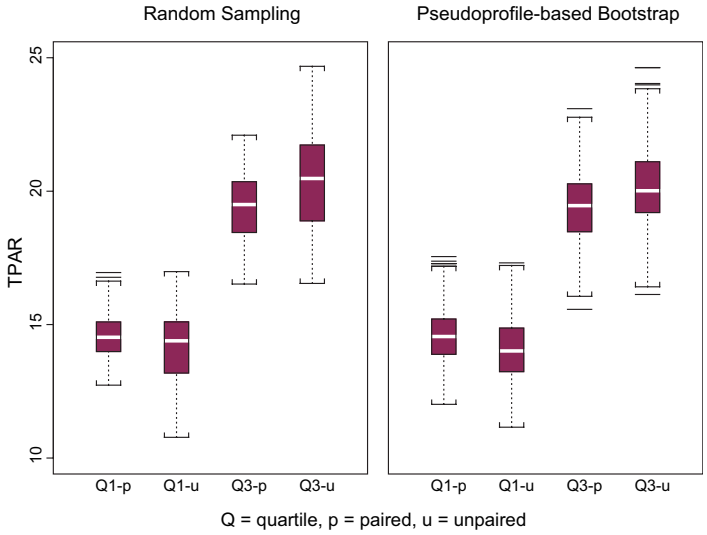

Figure 3. Comparison of the performance of the RS and PpbB approaches when TPAR is computed from paired and unpaired data. The comparison is focused on distribution of the first and third quartiles (Q1 and Q3, respectively) of TPARs.

PpbB and RS Approaches

Paired Versus Unpaired

Figure 2 illustrates the results obtained with RS approach using paired and unpaired data at different replication levels (ie, M_1 equals 10, 100, and 500 to build up the population pool). This was then followed by a calculation of TPAR over M_2 (ie, 50) virtual studies (with N = 18 for each study). Across all 3 population pool levels (ie, M_1 = 10, 100, and 500), paired observations consistently yielded tighter distributions than unpaired ones. Similar results were obtained with the PpbB approach.

If a drug is designed to target a particular tissue, the interest might be in having a minimal target TPAR. In that case, having knowledge of mean TPAR would not be enough. Having knowledge of the distribution of TPAR across virtual studies (ie, replicates) in terms of the summary statistics (first quartile Q_1, mean, median, third quartile Q_3) becomes valuable. Thus, knowing that the TPAR is not below a certain cut off, such as the first quartile of the TPAR distribution would be important. To provide such an insight, we examined the distribution of TPAR within and between replicates and have provided a summary of the distribution of TPAR across virtual studies. Consequently, Figure 3 provides an amplification of the outcomes with the 2 approaches when the first and third quartiles (Q1 and Q3, respectively) for paired and unpaired data are compared. The quartiles for the unpaired data have a wider spread, with the lower adjacent value of the distribution of Q1 values in the box plot extending beyond that for paired data in both RS and PpbB approaches. Disrupting the correlation structure in the data by unpairing the data yielded more variable results than when the correlation structure in the data was maintained by pairing. Thus, breaking the correlation structure between tissue and plasma observations resulted in a loss of information. Therefore, the rest of the study is focused on the paired scenario only.

A tabular comparison of the results obtained with the RS and PpbB approaches are shown in Table 5. In addition to the typical fashion of only describing distribution of mean of TPAR, Table 5 also includes distributions of quartiles of TPAR in terms of Q1 and Q3 with associated standard errors. The resampling approaches yielded comparable results when the number of replications was at least 600 with mean TPAR around 17, but the RS approach converged faster than the PpbB approach. (See the ‘‘Convergence’’ section below for more details.)

Convergence

An empirical method was used in monitoring convergence. To examine the effect of the number of replications (ie, M_1 in RS and B_1 in PpbB), a graphical presentation of percentage change (PC) of mean TPAR is shown in the middle panel of Figure 4 and Figure 5 for the RS and PpbB approaches, respectively. In addition, the PC of Q1 and Q3 are also plotted in the left and right panels of each figure. The acceptable range for the percentage change is calculated from summary statistics/confidence intervals of PC across all replication levels considered (ie, from M_1 with as little as 5 replications to as high as 1000 replications), and for statistics Q1, mean, and Q3. This range was determined by visual inspection of the convergence graphs with the assumption that over the range of the replications, the PC trend should be stabilized with limited amount of fluctuations. Therefore, the percentile cut-off range was chosen using a trimming approach, and the range of percentiles 12.5 and 87.5 was found to be appropriate for both sampling approaches and across the 3 summary statistics. Figure 4 shows the convergence trend for the RS approach. For all 3 statistics (Q1, mean, and Q3) of interest, 100 replications are sufficient. On the other hand, the number of replications needed for the distributions of summary statistics of TPAR with the PpbB is at least 600 replications (see Figure 5), owing to the instability in Q1. The range for the RS approach is considerably tighter than that for the PpbB approach. In fact, the range of PC is −1.28% to 1.56% for the RS approach, and −2.26% to 5.10% for the PpbB approach. This finding indicated that there was a larger variability in TPAR estimates obtained with the PpbB approach when compared with that obtained using the RS approach. The uniqueness of the RS approach lies in the population sampling pool, which is populated by generating M_1 replications through resampling concentra-

Table 5. Distribution of Tissue-to-Plasma AUC Ratio Parameter Estimates Obtained Using Random Sampling (left panel) and Pseudo-profile-based Bootstrap (right panel) Approaches*

Random Sampling Approach						
Tissue-to-Plasma AUC Ratios						
	Q1		**Mean**		**Q3**	
†**Repl**	**Mean**	**(SE)**	**Mean**	**(SE)**	**Mean**	**(SE)**
5	14.31	(0.94)	16.64	(0.88)	18.64	(1.45)
10	15.01	(0.95)	17.51	(0.85)	19.80	(1.29)
50	14.46	(1.00)	17.17	(0.95)	19.33	(1.48)
100	14.75	(0.96)	17.28	(0.82)	19.38	(1.21)
200	14.57	(0.99)	17.15	(0.84)	19.35	(1.26)
300	14.83	(1.01)	17.39	(0.90)	19.71	(1.32)
400	14.34	(1.12)	17.08	(0.95)	19.28	(1.46)
500	14.49	(0.89)	17.16	(0.84)	19.48	(1.36)
600	14.53	(1.08)	17.13	(0.91)	19.28	(1.17)
700	14.61	(1.05)	17.25	(0.97)	19.53	(1.38)
800	14.84	(0.99)	17.41	(0.84)	19.61	(1.20)
900	14.75	(1.05)	17.24	(0.89)	19.49	(1.24)
1000	14.43	(1.01)	17.09	(0.87)	19.41	(1.35)
Pseudoprofile-based Bootstrap						
Tissue-to-Plasma AUC Ratios						
	Q1		**Mean**		**Q3**	
‡**Repl**	**Mean**	**(SE)**	**Mean**	**(SE)**	**Mean**	**(SE)**
5						
10	14.43	(0.42)	15.76	(0.41)	17.15	(1.10)
50	14.05	(0.75)	16.71	(0.83)	18.70	(1.09)
100	15.12	(0.93)	17.93	(0.68)	20.36	(0.95)
200	14.45	(1.15)	17.02	(0.85)	19.07	(1.20)
300	14.63	(0.94)	17.16	(0.87)	19.20	(1.34)
400	14.89	(0.93)	17.27	(0.80)	19.35	(1.16)
500	14.28	(0.85)	17.08	(0.78)	19.54	(1.29)
600	14.57	(0.96)	17.30	(0.80)	19.76	(1.19)
700	14.34	(1.09)	17.05	(0.88)	19.38	(1.33)
800	14.90	(1.02)	17.44	(0.91)	19.77	(1.25)
900	14.50	(0.94)	17.12	(0.84)	19.32	(1.34)
1000	14.53	(1.02)	17.18	(0.78)	19.43	(1.17)

*Q1 and Q3 refer to the first and third quartiles of distribution of TPAR. AUC indicates area under the curve; and Repl, replication.
†Replication is $M1$ (ie, the number of replicates for each subject in Phase 1 of the RS approach).
‡Replication represents B_1 replicates used in the PpbB approach.

tion time profiles for each subject (ie, in this study with N = 18 animals, 100 replications for each animal is equivalent to total of 1800 [=18 × 100 distinct PK profiles in the population sampling pool). Secondly, M_2 copies of virtual studies are sampled from the population sampling pool to derive a distribution for any function of interest.

Outlier Effect on Robustness

Figure 6 shows the distribution of mean TPAR obtained from simulating 50 replicates (ie, $M_2 = 50$) of the base data set with the value of one tissue concentration value inflated to create an outlier in each replicate. The effect of one

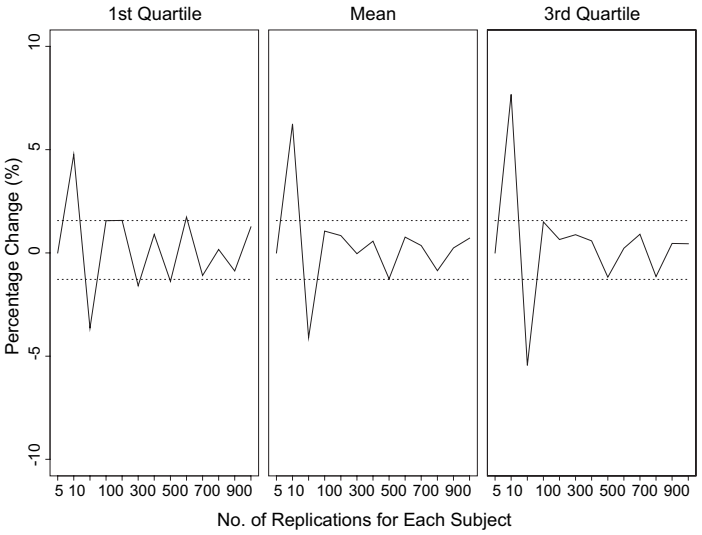

Figure 4. Convergence trend monitoring using percentage change in summary statistics (Q1, mean, and Q3) of tissue-to-plasma AUC ratios estimates obtained by the random sampling approach.

outlier can be measured by how big the distance is from the original mean TPAR value of ∽17 (see Table 5). The naive averaging approach performed the worst of all 3 approaches, and PpbB had a wider spread than the RS approach. In Figure 6, it appears that the distribution of TPAR estimates obtained with the naive averaging approach was the tightest. It has to considered that by the very nature of the naive averaging approach variability has been eliminated, hence the results. When the scenario for 2 outliers was considered, Figure 7 illustrates the effect when 2 tissue concentration values were randomly selected to create outliers in each replicate by calculating the PC from mean TPAR of 17 across the 3 methods, given the 4 levels of outlier perturbation (ie, 10%, 20%, 30%, or 40% increase in concentration values). Clearly, the RS approach provides results that are more robust than the other 2. The bias in the estimation of TPAR is more prominent with the PpbB and naive averaging approaches than with the RS approach (Figure 7).

DISCUSSION

We investigated a nonparametric random sampling approach that we are proposing for the estimation of robust TPAR and compared it with the PpbB and naive averaging approaches. Also, the estimation of tissue-to-plasma ratio using the independent time points approach was examined. It is obvious from Tables 2 and 3 that estimating tissue-to-plasma ratio independently at various times is a very unreliable method, since various ratios are obtained at various time points and it is unclear which of the ratios to choose. Also, it is impossible to compute ratios when samples from a particular biological matrix are below the limit of quantitation or are unquantifiable. The independent time points approach for calculating tissue-to-plasma ratio should, therefore, be avoided. Although the naive data averaging approach for computing AUC provides a single AUC value for drug exposure in each of the 2 matrices and consequently a single value of TPAR, the correlation in the data structure is unaccounted for and there is no measure of variability or uncertainty around the estimates. With this method, when concentrations are below the limit of quantification they are ignored in the calculation of the mean concentration at the particular time point. The mean concentration is calculated only with available data. Thus, the mean profile obtained in such a situation does not represent the actual mean profile since mean concentrations at each time point are not calculated from equal number of time points. These drawbacks not withstanding, the approach is better than the independent time points approach. However, both approaches are inferior to the resampling approaches—PpbB and RS.

Breaking the correlation structure between tissue and plasma observations results in a loss of information when using any of the resampling approaches. Therefore, it is important to maintain the correlation structure in paired data sets used in estimating TPAR. By doing this, variability in the calculated TPAR is minimized.

Although there are similarities in the TPAR estimates produced by the PpbB and RS approaches, the latter converges faster than the former. Convergence is achieved with only 100 replications (ie, $M_1 = 100$) per subject with the RS approach, while at least 600 bootstrap (ie, $B_1 = 600$) replications is required for the PpbB approach. In general, 100 replications are adequate in the first phase of the RS

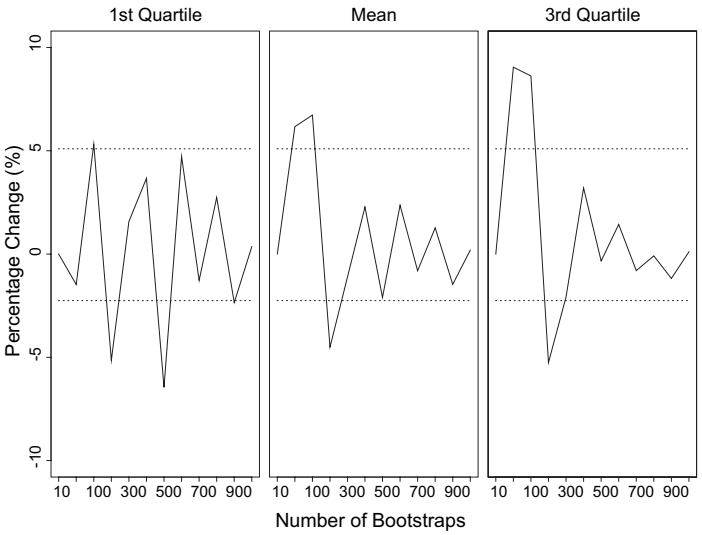

Figure 5. Convergence trend monitoring using percentage change in summary statistics (Q1, mean, and Q3) of distribution of tissue-to-plasma AUC ratios estimates obtained by the PpbB approach.

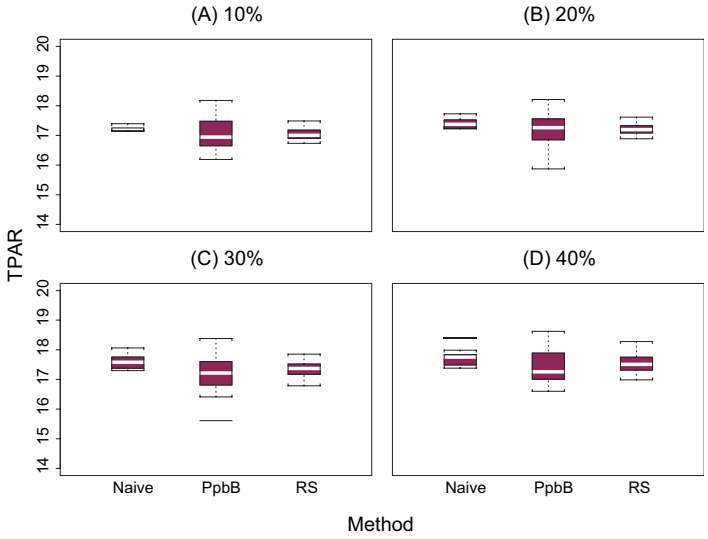

Figure 6. The effect of outlier on distribution of TPAR when inflating one concentration by (A) 10%, (B) 20%, (C) 30%, or (D) 40% using the naive averaging (naive), PpbB, and RS approaches.

approach for robust estimation of TPAR. Also, the acceptable range for TPAR estimates is narrower for the RS approach (Figure 4) when compared with the PpbB approach (Figure 5). Thus, the PpbB approach requires a larger number of replications to yield robust estimates. The difference lies in the 2-phase—population and study level—sampling of the RS approach. The tightness of the distribution of estimates obtained with the RS approach can be attributed to the creation of the representative population sample pool for subsequent study level sampling of parameters of interest. This is a unique feature of the RS approach. Also, the estimation of TPAR by the RS approach is not affected by missing data or imbalance in the number of concentrations at each time point over the sampling duration. Individual PK profiles are generated by sampling from available data at each time point across time points. Similarly, the PpbB approach is not affected by missing data or data imbalance.

When the effect of outliers on robustness was investigated, the naive data averaging approach performed the worst, while the RS approach performed the best. The edge that the RS approach has over the PpbB approach is, again, owing to the 2-phase nature of implementation of the methodology. The robustness of the RS approach lies in the creation of the population sample pool before the study level sampling for the estimation of TPAR. Also, the greater bias obtained with the PpbB approach when compared with the RS approach is probably due to the fact that mean parameter estimates obtained from bootstrap replicates may be influenced by data in the tails of the distribution.[6]

CONCLUSION

We have compared traditional approaches used in the estimation of TPAR with the PpbB approach and with the RS approach that we have proposed. The traditional approaches—independent time points and naive data averaging approaches—are inferior to the sampling/resampling approaches. The RS approach performed better than the

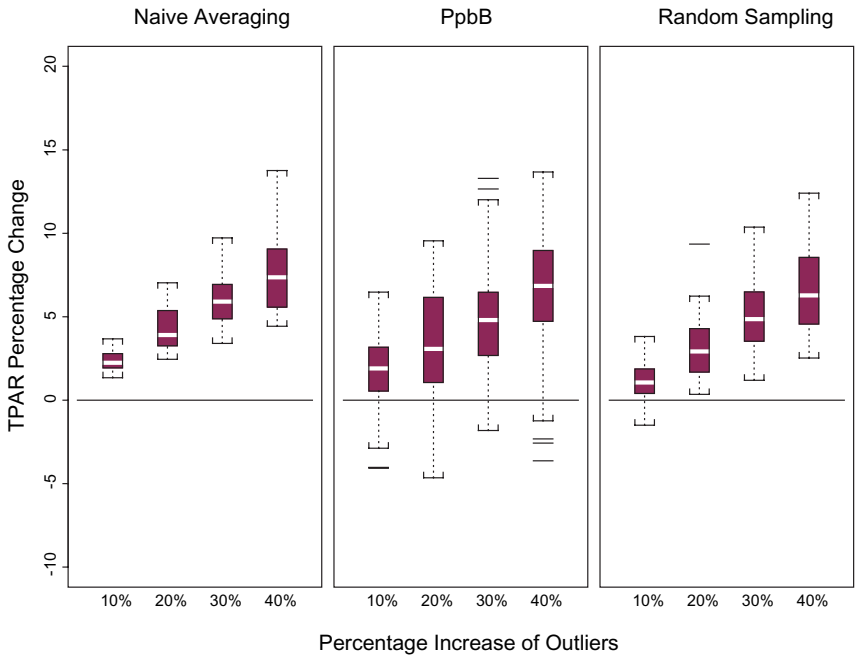

Figure 7. The effect of outlier based on the percentage increase distribution of TPAR when inflating 2 concentrations by 10%, 20%, 30%, or 40% using the naive averaging (left panel), PpbB (middle panel), and RS (right panel).

PpbB approach because of its unique algorithm. Also, fewer replications are required for robust estimation of TPAR. The computer intensive methods provide estimates of TPAR with measures of dispersion and uncertainty. The RS approach is therefore recommended as the method of choice for obtaining robust estimates of TPAR, when analyzing extremely sparsely sampled data.

REFERENCES

1. Lindstrom FT, Birkes DS. Estimation of population pharmacokinetic parameters using destructively obtained data: a simulation study of the one compartment open model. *Drug Metab Rev*. 1984;15:195-264.

2. McArthur RD. Parameter estimation in a two compartment population pharmacokinetic model with destructive sampling. *Math Biosci*. 1988;91:157-173.

3. Mager H, Goller G. Resampling methods in sparse sampling situations in preclinical pharmacokinetic studies. *J Pharm Sci*. 1998;87:372-378.

4. Efron B. Bootstrap methods: another look at the jackknife. *Ann Statist*. 1979;7:1-26.

5. Jones CD, Sun H, Ette EI. Designing cross-sectional pharmacokinetic studies: implications for pediatric and animal studies. *Clin Res Regul Affairs*. 1996;13(3&4):133-165.

6. Ette EI, Onyiah LC. Estimating inestimable standard errors in population pharmacokinetic studies: the bootstrap with winsorization. *Eur J Drug Metab Pharmacokinet*. 2002;27:213-224.